JOURNAL OF SOLID STATE CHEMISTRY **41**, 253–261 (1982)

Optical Transition Probabilities of Er^{3+} in Fluoride Glasses*

R. REISFELD† AND G. KATZ

Department of Inorganic and Analytical Chemistry, Hebrew University, Jerusalem, Israel

N. SPECTOR

Soreq Nuclear Research Center, Yavne, Israel

C. K. JØRGENSEN

Département de Chimie minérale, analytique et appliquée, University of Geneva, Switzerland

AND C. JACOBONI AND R. DE PAPE

Laboratoire des Fluorures et Oxyfluorures Ioniques (E.R. CNRS No. 609), Université du Maine, F-72017 Le Mans Cedex, France

Received August 5, 1981; in final form October 5, 1981

Lead-based fluoride glasses of the system PbF_2–GaF_3–MF_2(M = Zn or Mn) doped by trivalent erbium were prepared by melting and quenching of the appropriate fluorides under inert atmosphere. Optical spectra of the glasses with and without manganese reveal identical characteristics in the near ir region of the spectrum. In the near uv and visible part, the manganese-containing samples show higher oscillator strength, probably due to interaction between Mn^{2+} and Er^{3+}. Radiative and nonradiative characteristics of the glasses were computed, using the Judd–Ofelt method. Laser transitions of the glasses were predicted.

1. Introduction

The group in Le Mans has found several types of lead-containing fluoride glasses (*1*, *2*) in definite intervals of composition. The visible absorption spectra of the colored examples allow conclusions to be made about the local symmetry of transition-group ions containing a partly filled *d* shell (*1*) or *f* shell (*3*), and also about their oxidation state (*4*). In this paper, we report the absorption spectra of the $4f^{11}$ system trivalent erbium, in some of the samples coexisting with bivalent manganese, a well-understood $3d^5$ system. In a following paper, we are going to discuss the luminescence of such systems. The general behavior of erbium in vitreous materials, and the Judd–Ofelt theory of intensities of absorption bands (*3*, *5*) and of transition probabilities of luminescence, has been reviewed (*6*, *7*).

---

* Partially supported by U.S. Army Contract DAJA-80-C-O.188.

† Enrique Berman Professor of Solar Energy.

0022-4596/82/030253-09$02.00/0

Whereas most previously studied glasses (silicate, borate, phosphate, germanate, tellurite, etc.) have oxygen directly adjacent to transition-group ions, careful exclusion of humidity allows the preparation of fluoride glasses having fluorine bound to the cations (*1*).

Another difference from the conventional glasses (consisting of mixed oxides) is that the distinction between network formers (the relatively small atoms B, Si, P, Ge, etc., forming highly polymeric oxygen-bridged anions, frequently having a local symmetry close to that of a regular tetrahedron) and network modifiers (large cations such as lead, barium, calcium, alkaline metals, etc.), introducing themselves in available cavities and loosely connecting a relatively large number of oxygen neighbor atoms, is not directly applicable to our lead-containing fluoride glasses. The spectroscopic work (*1*) on bivalent cobalt and nickel and on trivalent vanadium and chromium demonstrated local octahedral symmetry, and it is highly probable that bivalent manganese and zinc, as well as trivalent gallium, also are octahedral. In a sense, we have octahedral network formers (rather than tetrahedral). It is beyond doubt, however, that the absorption bands of erbium in fluoride glasses are so intense that the local symmetry is removed considerably from that of a regular octahedron, and indeed, far from any situation having a center of inversion. Actually, only a minor part of all lanthanides in crystalline phases are situated on sites possessing a center of inversion (such as is known from the rather exceptional cases of $ErCl_6^{3-}$, the quarter of erbium in C-type Er_2O_3 on sites of S_6 (and not C_2) symmetry, and the cubic pyrochlore $Er_2Ti_2O_7$). It was recently reviewed (*8*) how the trivalent lanthanides assume varying symmetries and differing coordination numbers N (frequently 7, 8, 9, and 10). The absorption bands of the erbium ions in the fluoride glasses are remarkably narrow, and suggest a small degree of nonequivalence in local environment (in contrast to erbium and other lanthanides in conventional glasses, showing heterogeneous dispersion as network modifiers (*3*) by inhomogeneous line broadening). Having N higher than 6 (often 9 in crystalline fluorides), erbium maintains a role intermediate between a network former (where it would be octahedral) and a modifier (where its behavior would provide broader absorption bands).

Another characteristic of fluoride glasses (*9*) is a very low absorption in the far infrared (allowing hopes of making optical fibers with weak Rayleigh scattering), concomitant with low vibrational frequencies (which are a major condition for low multiphonon deexcitation, competing with luminescence). Actually, it is possible to predict feasible laser materials (*3*) by experimental evaluation of these phonon energies and of the Judd–Ofelt parameters.

2. Experimental

The glasses were obtained by heating the mixtures of anhydrous fluorides in a platinum crucible between 600 and 900°C in a dry box in an anhydrous atmosphere consisting mainly of nitrogen. The melt was cast in a bronze mold heated to 230°C and annealed for 1 hr.

The composition of the glasses was chosen in analogy to glasses (*1*) formed by PbF_2, MnF_2, and FeF_3. In this report we discuss the two kinds, (A) and (B), obtained by adding 2 wt% ErF_3 to mixtures otherwise having the composition in mole%:

(A) 46 PbF_2 : 22 MnF_2 : 30 GaF_3 : 2LaF_3,
(B) 46 PbF_2 : 22 ZnF_2 : 30 GaF_3 : 2LaF_3.

The density and refractive index for (A) is 6.0 g/cm^3 and 1.637 and for (B) 6.05 g/cm^3 and 1.611. The samples were polished into the shape of parallelepipeds, (A) with the dimensions 11.7 × 3.7 × 2.6 mm and (B)

11.5 × 3.2 × 2.2 mm. The absorption spectra were measured at room temperature (relative to air) on a Cary 14 spectrophotometer between 250 and 1700 nm. Close to 280 nm, there is a large absorption peak due to the first excited configuration $6s6p$ of lead (*3*, *4*).

The absorption spectra of the two glasses are identical in band positions and intensities in the infrared region above 700 nm, whereas the bands due to erbium are perceptibly stronger in the manganese-containing glass (A) below 700 nm. This effect may be related (*10*) to antiferromagnetic coupling in ErFMn bridges. Further on, the glass (A) shows two narrow bands at 398 and 334 nm due to bivalent manganese, as well as a broad band between 430 and 550 nm. It is likely that the two peaks are due to the coinciding excited levels ($^4A_1$, ^4E) and the second ^4E of octahedral MnF_6^{4-}, but it is also conceivable that the two bands correspond to other levels derived from ^4G and ^4D (of $3d^5$) in another symmetry. A comparison of the absorption spectra of the two glasses and of the fluorite-type (so-called stabilized cubic zirconia) $Zr_{0.498}Y_{0.498}Er_{0.0038}O_{1.749}$ (*11*) is shown in Fig. 1.

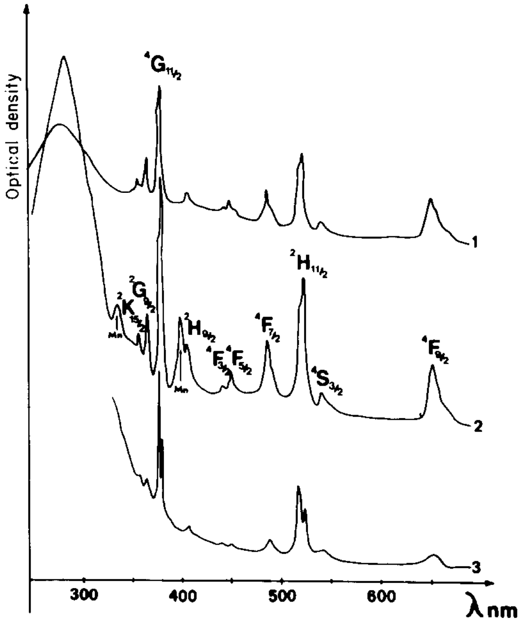

FIG. 1. Absorption spectra of Er^{3+}-doped fluoride glasses and Er^{3+}-doped ZrO_2 (Y_2O_3). 1—2 wt% ErF_3: 46 PbF_2, 22 ZnF_2, 30 GaF_3, 2 LaF_3 (mol%), t = 2.2 mm. 2—2 wt% ErF_3: 46 PbF_2, 22 MnF_2, 30 GaF_3, 2 LaF_3 (mol%), t = 2.6 mm. 3—0.55 wt% Er_2O_3: 67 ZrO_2, 33 Y_2O_3 (mol%), t = 2.95 mm.

3. Theoretical

The calculations of the eigenvectors and the radiative transition probabilities were performed as described in Ref. (*3*). The oscillator strength is obtained from the area of the absorption band on a wavenumber (ν') scale

$$f = 4.318 \times 10^{-9} \int \epsilon(\nu')d\nu', \qquad (1)$$

where ϵ is the molar extinction coefficient.

The first step in the theoretical calculation is the evaluation of the free-ion eigenvectors. According to the Judd–Ofelt (JO) theory, the free-ion wavefunctions are combined with the $|U^{(t)}|^2$ matrix elements (indicating the perturbation of the configuration containing the partly filled $4f$ shell by the surrounding atoms) to give the transition probability. The calculated J levels of the free ion are adjusted by least squares to the levels observed in the condensed material. Such calculations of eigenvectors have been performed by Weber (*12*) for Er^{3+} in LaF_3 (also studying transitions between excited J levels) and Krupke and Gruber (*13*) previously calculated energy levels of the same material using Slater parameters F^k of interelectronic repulsion (or the equivalent Racah parameters E^k) and the spin–orbit parameters ζ_f. We have introduced also the α (Trees), β (Q group), and γ (Casimir) corrections, and the results for these seven parameters are given in Table I.

The J eigenvalues obtained from these parameters are then used to calculate the doubly reduced matrix elements of the unit tensors $U^{(t)}$ (with t = 2, 4, 6) in the JO

TABLE I

RADIAL PARAMETERS FOR $4f^{11}$ (TRIVALENT ERBIUM) IN FLUORIDE GLASSES

Parameter	Value (cm^{-1})
A	103,900
F_2	444
F_4	64.6
F_6	6.85
α	34
β	−914
γ	1800
ζ	2395

expression for the forced electric dipole line strength S_{ed}. It may be noted that the squares of the intensity matrix elements $|U^{(t)}|^2$ agree within 2% with the calculations by Weber (*12*) for $Er_xLa_{1-x}F_3$ and by Krupke (*14*) for Er_2O_3, as further analyzed by Rahman (*15*):

$$S_{\text{ed}} = e^2 \sum_{t=2,4,6} \times \Omega_t (f^N[\gamma SL]J \| U^{(t)} \| f^N[\gamma' S' L']J')^2. \quad (2)$$

The same eigenvectors are used in calculating the magnetic dipole line strength,

$$S_{\text{md}} = (e^2 h^2/4m^2c^2) \times |\langle f^N[\gamma SL]J \| L + 2S \| f^N[\gamma' S' L']J' \rangle|^2. \quad (3)$$

The total oscillator strength f of a transition at the frequency ν is given by

$$f(\gamma J; \gamma' J') = \frac{8\pi^2 m\nu}{3h(2J+1)} \times \left[\frac{(n^2+2)^2}{9n} S'_{\text{ed}} + nS'_{\text{md}}\right], \quad (4)$$

where n is the refractive index of the glass, and $S' = S/e^2$ for both electric and magnetic dipoles and is given in units of square centimeters. The total radiative transition probability is given by

$$A(\gamma J; \gamma' J') = [(64\pi^4\nu^3 e^2/3hc^3)(2J+1)] \times [(1/9)n(n^2+2)^2 S_{\text{ed}} + n^3 S_{\text{md}}]. \quad (5)$$

This radiative transition probability is then used to calculate the integrated induced emission cross section

$$\sigma_{\text{p}}\,\Delta\nu' = \int \sigma(\nu')d(\nu'). \quad (6)$$

When $\lambda_{\text{p}} = (1/\nu')$ is the wavelength of the fluorescent peak and $\Delta\nu'$ is the effective fluorescence linewidth determined from the fluorescence lineshape, the peak cross section σ_{p} is given (*16*) by

$$\sigma_{\text{p}}(\lambda) = \lambda^4 A/(8\pi c n^2 \Delta\lambda) \quad (7)$$

and the branching ratio β_{12} is $A(J_1, J_2)/\Sigma_n A(J_1, J_n)$.

The multiphonon relaxation rate between two J levels in glasses may be adequately described (*3*) by a single phonon frequency model by the formula

$$W_{\text{NR}} = [B \exp(-\alpha \Delta E)][n(\omega, T) + 1]^p, \quad (8)$$

where B and α are constants characteristic of the host material, ΔE is the energy gap between the emitting and the closest lower electronic level, ω is the stretching frequency of the glass-forming groups, and $p = \Delta E/\hbar\omega$ is the number of phonons which must be emitted in order to conserve energy during the transition. The stretching frequencies for the fluoride glasses have been estimated to $\hbar\omega$ close to 500 cm^{-1} ($\alpha = 0.007$ and $B = 4 \times 10^9$) by comparison with zirconium fluoride glasses (*17*). The exact values will be evaluated using Raman spectra.

The explicit temperature dependence of W_{NR} through the Bose–Einstein occupation number $n = 1/[\exp(\hbar\omega/kT) - 1]$ provides a way to determine the number and energy of the phonons involved in the decay processes.

The multiphonon relaxation rates W may be obtain from the measured life times τ_{obs} and the calculated radiative transition probabilities using the relation

$$W = 1/\tau_{\text{obs}} - \Sigma A \quad (9)$$

or from measurements of the quantum yield

η using

$$\eta = \Sigma A/(\Sigma A + W). \tag{10}$$

α is connected with the coupling constant ϵ by

$$\alpha = -\ln(\epsilon)/\hbar\omega. \tag{11}$$

The parameters α, ϵ, and B are dependent on the host material but roughly independent of the specific J level of a given lanthanide (and to a certain approximation even independent of the lanthanide). Using Eq. (8) and assuming a weak temperature dependence for frequencies of 500 cm^{-1}, multiphonon decay rates can be obtained at room temperature (*18*).

4. Results

(*a*) *Absorption Spectra*

Figure 1 shows the absorption spectra in the range 300 to 700 nm of Er^{3+} in the two fluoride glasses compared with cubic stabilized zirconia crystals (*11*). It should be noted that, while in general the absorption peaks in the zirconia crystal are lower, in the case of the hypersensitive transition $^4I_{15/2} \rightarrow {}^2H_{11/2}$ the maxima are comparable. For the other hypersensitive transition, $^4I_{15/2} \rightarrow {}^4G_{11/2}$, the intensity in the manganese-doped glass is significantly higher, compared to the zirconia crystal and the zinc-doped glass. The peak intensities of the latter transition increase in the order zinc glass, zirconia, and manganese glass. A perceptible influence of manganese ions is known (*19*) from the cubic perovskite $RbMnF_3$ containing traces of Er^{3+} (each forming six ErFMn bridges).

(*b*) *Oscillator Strengths*

The measured and calculated f values are presented in Table II. In column 1, we give the excited J levels, and in columns 2 and 3 the wavenumbers and wavelengths of the transition. In columns 4, 5, and 6 we give, respectively, the observed oscillator strength, the least-squares adjusted values

TABLE II

COMPARISON OF EXPERIMENTAL AND CALCULATED OSCILLATOR STRENGTHS OF Er^{3+} IN PbZnGaLa FLUORIDE GLASS

			$f \times 10^6$		
				Least squares	
Transition	Energy (cm^{-1})	Transition wavelength (nm)	Observed	Adjusted (Eq. (2))	Calculated (Eq. (4))
$^4I_{15/2} \rightarrow {}^4I_{13/2}$	6,527	1532	2.01	1.203	1.69
$^4I_{11/2}$	10,277	973	0.67	0.521	0.51
$^4I_{9/2}$	12,484	801	0.32	0.256	0.25
$^4F_{9/2}$	15,384	650	1.76	1.757	1.72
$^4S_{3/2}$	18,552	539	0.41	0.483	0.465
$^2H_{11/2}$	19,193	521	2.78	3.179	3.015
$^4F_{7/2}$	20,618	485	1.25	1.859	1.83
$^4F_{5/2}$	22,321	448	0.634	0.584	0.577
$^4F_{3/2}$	22,727	440	0.35	0.339	0.207
$^2H_{9/2}$	24,691	405	0.56	0.708	0.713
$^4G_{11/2}$	26,385	379	5.805	5.595	5.81
$^2G_{9/2}$	27,548	363	1.34	1.145	1.15
$^2K_{15/2}$	28,169	355	0.52	0.359	0.409

TABLE III

INTENSITY PARAMETERS Ω_t (IN THE UNIT 10^{-20} cm^2) OF Er^{3+} IN ZINC-CONTAINING FLUORIDE GLASS AND IN VARIOUS OTHER MATERIALS

	Ω_2	Ω_4	Ω_6
$Er_{0.020}Pb_{0.451}Zn_{0.215}Ga_{0.294}La_{0.020}F_{2.334}$	1.54 ± 0.25	1.13 ± 0.40	1.19 ± 0.20
$Er_xY_{2-x}O_3$ crystal (*14*)	4.59 ± 0.25	1.21 ± 0.21	0.48 ± 0.33
$Er_{0.0088}Y_{0.498}Zr_{0.498}O_{1.745}$ crystal (*11*)	2.92 ± 0.17	0.78 ± 0.27	0.57 ± 0.14
$LiErP_4O_{12}$ crystal (*20*)	0.85 ± 0.09	0.96 ± 0.19	0.72 ± 0.09
ErP_5O_{14} crystal (*20*)	1.68 ± 0.17	2.07 ± 0.12	0.98 ± 0.21
Er^{3+} aqua ion, solution (*21*)	1.59 ± 0.13	1.95 ± 0.19	1.90 ± 0.10
$ErW_{10}O_{35}^{-7}$, solution (*5*)	6.7 ± 0.5	2.3 ± 0.3	1.4 ± 0.2

evaluated from Eq. (2), and the values obtained from Eq. (4) for the zinc-containing glass using the refractive index 1.611. The background (see Fig. 1) is more difficult to subtract in the manganese-containing glass.

The three JO parameters Ω_t (obtained by least-squares fitting of our experimental oscillator strengths to the $|U^{(t)}|^2$ matrix elements) are given in Table III, together with recent data (*20*) for $LiErP_4O_{12}$ and ErP_5O_{14} and values for *C*-type Er_2O_3 according to Krupke (*14*) and further reviewed by Rahman (*15*), as well as the Er^{3+} aqua ion (*21*) and the heteropolytungstate $ErW_{10}O_{35}^{7-}$ in solution (*5*).

It is worthwhile to note that the three Ω_t are phenomenological parameters for each material (usually measured at room temperature). It does not seem feasible (*5, 14, 15*) to evaluate these parameters from the radial wavefunction of the lanthanide, and a realistic model of the perturbations from the surrounding atoms. This problem can be seen from a different point of view. In the gaseous ion, some transitions between *J* levels of the configuration $4f^N$ are allowed as electric quadrupolar transitions with probabilities proportional to $|U^{(2)}|^2$. By the same token, other transitions are allowed as electric 16-polar transitions with intensities proportional to $|U^{(4)}|^2$, and again others as 64-polar transitions with probabilities proportional to $|U^{(6)}|^2$. However, as first pointed out by Broer, Gorter, and Hoogschagen in 1945, this mechanism is entirely inadequate insofar as the oscillator strengths of the quadrupolar transitions are intrinsically determined by $\langle r^2\rangle^2/\lambda^4$, whereas the 16-polar transitions are proportional to $\langle r^2\rangle^8/\lambda^{16}$ and the 64-polar transitions to $\langle r^2\rangle^{32}/\lambda^{64}$. These quantities might be perceptible in the X-ray region, where the square of the wavelength λ corresponding to the transition considered is not much larger than the average $\langle r^2\rangle$ of the inner shell. However, they are truly microscopic in the visible region.

The empirical fact that the Judd–Ofelt theory works by comparing the highly overdetermined set of linear combination of the type in Eq. (2) with the observed oscillator strengths (cf. the uncertainties given in Table III) can be expressed in the more constructive way that, e.g., 256-polar transitions do not need to be considered. This is one out of many indications (*22, 23*) that $l = 3$ remains an appropriate description of the *J* levels of $4f^N$ in condensed matter. There are minor details where the Judd–Ofelt theory is not quite satisfactory, such as several transitions in trivalent europium (*17*), mainly dependent on Ω_2, and the worst case being the unexpected high intensity of $^3H_4 \rightarrow {}^3P_2$ in trivalent praseodymium (*3, 5*). A rather ad hoc explanation (*23*) would involve configuration interaction between the ^3P terms of the two configurations $4f^2$ and $5d^2$ (both having

TABLE IV

SELECTED POSSIBLE LASER TRANSITIONS OF Er^{3+} IN PbZnGaLa FLUORIDE GLASSES

Transition	Wavelength (nm)	Radiative transition rate A (sec^{-1})	Branching ratio β	Peak cross section for stimulated $p(\lambda)$ (10^{-20} cm^2)	Emitting level multiphonon rate W (sec^{-1})
$^2H_{11/2} \rightarrow {}^4I_{15/2}$	521	2570	0.908	1.16	6.9×10^7
$^4S_{3/2} \rightarrow {}^4I_{15/2}$	539	1120	0.658	0.72	2.3
$^4F_{9/2} \rightarrow {}^4I_{15/2}$	650	1140	0.902	0.52	14.3
$^2H_{11/2} \rightarrow {}^4I_{13/2}$	790	153	0.054	—	6.9×10^7
$^4I_{9/2} \rightarrow {}^4I_{15/2}$	801	109	0.688	0.08	1.6×10^3
$^4S_{3/2} \rightarrow {}^4I_{13/2}$	832	486	0.286	—	2.3
$^4I_{11/2} \rightarrow {}^4I_{15/2}$	973	127	0.816	0.17	4.4×10^{-2}
$^2H_{11/2} \rightarrow {}^4I_{9/2}$	1491	51	0.018	—	6.9×10^7
$^4I_{13/2} \rightarrow {}^4I_{15/2}$	1532	143	1.000	—	0
$^4I_{11/2} \rightarrow {}^4I_{13/2}$	2667	28.5	0.184	—	4.4×10^{-2}
Additional transitions for consideration					
$^4G_{11/2} \rightarrow {}^4I_{15/2}$	379	9300	0.831	1.48	5.3×10^4
$^2H_{9/2} \rightarrow {}^4I_{15/2}$	405	1210	0.450	—	8.4×10^3
$^4F_{3/2} \rightarrow {}^4I_{15/2}$	440	1260	0.498	0.32	3.4×10^8
$^4F_{5/2} \rightarrow {}^4I_{15/2}$	448	1340	0.493	0.24	5.0×10^4
$^4F_{7/2} \rightarrow {}^4I_{15/2}$	485	2700	0.799	1.53	3.3×10^5
$^4G_{11/2} \rightarrow {}^4I_{13/2}$	504	1430	0.128	—	5.3×10^4
$^2H_{9/2} \rightarrow {}^4I_{13/2}$	551	1100	0.409	—	8.4×10^3
$^4G_{11/2} \rightarrow {}^4I_{9/2}$	719	95.4	0.009	—	5.3×10^4
$^2H_{9/2} \rightarrow {}^4I_{11/2}$	694	271	0.101	—	8.4×10^3
$^4G_{11/2} \rightarrow {}^4F_{9/2}$	909	223	0.020	—	5.3×10^4

even parity). The reason why JO parameters are more successful for Ho^{3+}, Er^{3+}, and Tm^{3+} at the end of the lanthanides may be the increasing validity of exact ($l = 3$) as a function of decreasing ratio between the average radius of the 4*f* shell and the internuclear distance to the adjacent atoms.

Much of the interest in Judd–Ofelt theory has concentrated on pseudoquadrupolar hypersensitive transitions (*24*, *25*) where the transition probability increases strongly if the material parameter Ω_2 increases, since the squared matrix element $|U^{(2)}|^2$ is large. Among the largest Ω_2 values known, halide vapors such as NdI_3, $CsNdI_4$, and $NdBr_3$ represent quite extreme cases. The vapor consisting of adducts of $ErCl_3$ with $AlCl_3$ or $GaCl_3$ (*26*) shows Ω_2 about ten times higher than the aqua ion in Table III.

It was previously pointed out (*3*) that solid fluorides and aqua ions show stronger (and comparable) Ω_4 and Ω_6 than Ω_2. In the unit 10^{-20} cm^2, Ho^{3+} in crystalline LaF_3 (*27*) shows $\Omega_2 = 1.16$, $\Omega_4 = 1.38$, and $\Omega_6 = 0.88$. These values are not very different from Er^{3+} in our fluoride glass (cf. Table III). The situation is more extreme for Nd^{3+} in LaF_3 (*15*), where $\Omega_2 = 0.35 \pm 0.14$, $\Omega_4 = 2.57 \pm 0.36$, and $\Omega_6 = 2.50 \pm 0.33$. We do not believe that it has been emphasized previously that compounds with rather weak hypersensitive transitions (low Ω_2) tend to show large Ω_6. Among the seven entries in Table III, five have the product of Ω_2 and Ω_6 between 1.6 and 3.0. Though this argument should not be construed to indicate a strict inverse proportionality between these two parameters, it is striking that oxides have very large Ω_2 and unusually small Ω_6, whereas Er^{3+} aqua ions and fluoride glass have comparable values of all three Ω_t. A similar reversal is observed (*17*) for Eu^{3+} in zirconium fluoride glass (0.93, 2.61, 2.17) and phosphate glass (4.12, 4.69, 1.83), with the three Ω_t in parentheses. The trend observed (*6*, *29*) in borate, phosphate, germanate, and tellurite glasses is Ω_t approximately twice the value for C-type oxides.

(*c*) *Radiative and Nonradiative Transition Rates*

The oscillator strengths of the transitions between any pair of levels, obtained from Eq. (4), and radiative transition probabilities, from Eq. (5), are calculated in the second paper of this series, together with the calculated branching ratios for luminescence down to the various lower-lying J levels, including the ground state. In order to choose transitions suitable for laser action we have selected, in Table IV, those transitions where the radiative transition rates are greater than 100 $\sec^{-1}$ and multiphonon relaxation rates not less than 20 (Eq. (8)) where the distance between the emitting level and the next lower level is greater than 3000 cm^{-1}. The latter requirement is needed in order to circumvent the nonradiative relaxation rates. These selected transitions are listed in Table IV in increasing order of wavelengths.

(*d*) *Cross Sections for Stimulated Emission*

In this work we were able to determine $\Delta\bar{\nu}$ experimentally from the absorption spectra for those transitions which terminate at the ground state. The peak cross sections (from formula (7)) for stimulated emission obtained for these selected transitions are also given in Table IV. A certain number of the transitions presented in Table IV have been observed experimentally (*28*, pp. 625, 631) in yttrium lithium fluoride (YLF)$YLiF_4$.

(*e*) *Thermalization*

In Er^{3+}-doped fluoride glass the ${}^4S_{3/2}$ and ${}^2H_{11/2}$ level separation ΔE, as obtained from the absorption spectra, is 640 cm^{-1}. Thus, at room temperature thermalization of the two levels occurs and the effective radiation transition probability of the two levels has to be calculated using the formula

$$A_{\text{eff}} = \frac{12\exp(-\Delta E/kT)\Sigma A({}^2H_{11/2}) + 4\Sigma A({}^4S_{3/2})}{12\exp(-\Delta E/kT) + 4}, \tag{12}$$

where $kT = 209\ cm^{-1}$, $\Sigma A({}^2H_{11/2}) = 2831\ \sec^{-1}$, $\Sigma A({}^4S_{3/2}) = 1702\ \sec^{-1}$, and the $A_{\text{eff}} = 2361\ \sec^{-1}$. Owing to the fast multiphonon relaxation rate $W = 6.9 \times 10^7\ \sec^{-1}$ of the ${}^2H_{11/2}$ level, the laser transition can be expected mainly from the ${}^4S_{3/2}$ level.

5. Conclusions

In the present paper we present the calculated spectroscopic characteristics of various Er^{3+} transitions in two multicomponent fluoride glasses which lead to a selection of possible candidates for laser performance. The long wavelength transitions at 2667, 1532, and 1491 nm may be of special interest as sources for optical waveguides. In this wavelength region the Rayleigh scattering is small and the optical losses negligible, thus making the proposed candidates significant for optical communications. The luminescent characteristics of the glasses are discussed in a second paper under elaboration using the parameters calculated here.

Acknowledgment

We would like to express our gratitude to the late Dr. Jean-Pierre Miranday, who initiated the fruitful collaboration between our four laboratories, and who expressed so much imagination in the new field of fluoride glasses.

References

1. J. P. Miranday, C. Jacoboni, and R. De Pape, *J. Non-Cryst. Solids* **43,** 393 (1981).
2. J. P. Miranday, C. Jacoboni, and R. De Pape, *Rev. Chim. Min.* **16,** 277 (1979).
3. R. Reisfeld and C. K. Jørgensen, "Lasers and Excited States of Rare Earths," Springer-Verlag, Berlin (1977).
4. C. K. Jørgensen, "Oxidation Numbers and Oxidation States," Springer-Verlag, Berlin (1969).
5. R. D. Peacock, *Struct. Bonding (Berlin)* **22,** 83 (1975).
6. R. Reisfeld and Y. Eckstein, *J. Chem. Phys.* **63,** 4001 (1975).
7. R. Reisfeld, L. Boehm, and N. Lieblich, *J. Lumin.* **10,** 193 (1975).
8. C. K. Jørgensen and R. Reisfeld, *Top. Curr. Chem.* **100** (1981).
9. J. P. Miranday, C. Jacoboni, and R. De Pape, French Patent No. 79.07785; E.P. 0 017566.
10. C. K. Jørgensen, "The Rare Earths in Modern Science and Technology" (G. J. McCarthy, J. J. Rhyne, and H. B. Silber, Eds.), Vol. 2, p. 607, Plenum, New York (1980).
11. E. Greenberg, G. Katz, R. Reisfeld, N. Spector, B. Bendow, and R. N. Brown, *J. Chem. Phys.*, in press.
12. M. J. Weber, *Phys. Rev.* **157,** 262 (1967).
13. W. F. Krupke and J. B. Gruber, *J. Chem. Phys.* **41,** 1225 (1964).
14. W. F. Krupke, *Phys. Rev.* **145,** 325 (1966).
15. H. U. Rahman, *J. Phys. C* **5,** 306 (1972).
16. R. Reisfeld, "Proceedings, International Conference on Lasers, New Orleans, December 1980, J. Soc. Opt. Quantum Electronics McLean, Virginia p. 349 (1981).
17. B. Blanzat, L. Boehm, C. K. Jørgensen, R. Reisfeld, and N. Spector, *J. Solid State Chem.* **32,** 195 (1980).
18. R. Reisfeld, "Radiationless Processes" (B. Di-Bartolo and V. Goldberg, Eds.), p. 489, Plenum, New York (1980).
19. M. V. Iverson and W. A. Sibley, *Phys. Rev. B* **21,** 2522 (1980).
20. W. Ryba-Romanowski, Z. Masurak, B. Jezowska-Trzebiatowska, D. Schultze, and C. W. Waligora, *Phys. Status Solidi A* **62,** 75 (1980).
21. W. T. Carnall, P. R. Fields, and K. Rajnak, *J. Chem. Phys.* **49,** 4412 (1968).
22. C. K. Jørgensen, *Israel J. Chem.* **19,** 174 (1980).
23. C. K. Jørgensen, "International Review of Chemistry" (A. D. Buckingham, J. M. Thomas, and B. A. Trush, Eds.), **1,** 225, Butterworths, London (1981).
24. C. K. Jørgensen and B. R. Judd, *Mol. Phys.* **8,** 281 (1964).
25. B. R. Judd, *J. Chem. Phys.* **70,** 4830 (1979).
26. G. N. Papatheodorou and R. W. Berg, *Chem. Phys. Lett.* **75,** 483 (1980).
27. M. J. Weber, B. H. Matsinger, V. L. Donlan, and G. T. Surrat, *J. Chem. Phys.* **57,** 562 (1972).
28. L. Esterowitz, R. E. Allen, M. R. Kruer, and R. C. E. Eckardt, "The Rare Earths in Modern Science and Technology" (G. J. McCarthy, J. J. Rhyne, and H. B. Silber, Eds.), Vol. 2, Plenum, New York (1980).
29. R. Reisfeld and Y. Eckstein, *J. Solid State Chem.* **5,** 174 (1972).